

---

## A City-scale Three-dimensional Macroscopic Fundamental Diagram: Simulation Findings

Nan Zheng, École Polytechnique Fédéral de Lausanne

Konstantinos Aboudolas, École Polytechnique Fédéral de Lausanne

Nikolas Geroliminis, École Polytechnique Fédéral de Lausanne

Conference paper STRC 2013

**STRC**

**13<sup>th</sup> Swiss Transport Research Conference**

Monte Verità / Ascona, April 24-26, 2013

# A City-scale Three-dimensional Macroscopic Fundamental Diagram: Simulation Findings

Nan Zheng  
Laboratory Urban Transport  
System,  
ENAC, École Polytechnique  
Fédérale de Lausanne (EPFL),  
GC C2 406, Station 18,  
1015 Lausanne

Phone: 021 69 32484  
Fax: 021 69 32479  
Email:  
nan.zheng@epfl.ch

Konstantinos Aboudolas  
Laboratory Urban Transport  
System,  
ENAC, École Polytechnique  
Fédérale de Lausanne (EPFL),  
GC C2 390, Station 18,  
1015 Lausanne

Phone: 021 69 32964  
Fax: 021 69 32479  
Email:  
konstantinos.ampountolas@epfl.ch

Nikolas Geroliminis  
Laboratory Urban Transport  
System,  
ENAC, École Polytechnique  
Fédérale de Lausanne (EPFL),  
GC C2 389, Station 18,  
1015 Lausanne

Phone: 021 69 32481  
Fax: 021 69 32479  
Email:  
nikolas.geroliminis@epfl.ch

## Abstract

Recent research has demonstrated that the Macroscopic Fundamental Diagram (MFD) is reliable and practical tool for modelling traffic dynamics and network performance in single-mode (cars only) urban road networks. In this paper, we first extend the modelling of the single-mode MFD to a bi-modal (bus and cars) one. Based on simulated data, we develop a three-dimensional MFD (3D-MFD) relating the accumulation of cars and buses, and the total circulating flow in the network. We propose an exponential function to capture the shape of the 3D-MFD, which shows a good fit to the data. Moreover, we derive a 3D-MFD for passenger network flows with the consideration of high passenger occupancy of the buses. The output of this paper is an extended 3D-MFD model that can be used to (i) monitor traffic performance and, (ii) develop various traffic management strategies in bi-modal urban road networks, such as redistribution of urban space among different modes, perimeter control, and bus priority strategies.

## Keywords

City-scale, Three-dimensional MFD (3D-MFD), Bimodal, Passenger flow

# 1. Introduction

To understand the physics of urban mobility, traffic dynamics of urban networks with multiple modes need to be analyzed under various network structures. As multiple modes compete for limited urban space, conflicts and interactions are developed resulting in congestion. Existing literature on multimodal traffic mainly focuses on design and operation of special lanes [1], [2], [3], [4], optimization of signal control [5], [6], [7] etc. However there is no significant body of work dedicated on the modeling of traffic dynamics and the influence of each mode on the network performance. Most of the existing body of work falls short either in the scale of application or the treatment of congestion dynamics (small scale and/or static models). For example, reference [2] estimates traffic state for each mode based on a BPR type [8] of model which works only for uncongested and static conditions. References [1], [3], [9] are based on the link-scale Fundamental Diagram, which can experience high scatter and therefore cannot provide accurate estimates of speed and travel time. These microscopic models are also computationally complex when applied at network scale. Macroscopic approach can overcome these problems with less cost. The idea of macroscopic traffic model for car-only urban networks has been initially proposed in [10] and was re-initiated later in [11], [12]. The demonstration of the existence with dynamic features and field data of the Macroscopic Fundamental Diagram (MFD) is recent [13]. Many recent works have focuses on the properties, analytical form and other observed phenomena of the MFD. We refer the readers to the following references [14]-[23]. Given the MFD of a network, effective traffic management strategies can be readily developed to mitigate congestion, examples including perimeter traffic flow control [24], [25] and cordon-based pricing [26].

Building in the knowledge of the single-mode MFD, developing and understanding the dynamics of multimodal network is promising. In this paper, we seek to extend the modelling and the application of the single-mode MFD to a bi-modal (bus and cars) one, with the consideration of passenger flows and traffic performance of each mode. The dynamics of traffic flow in a bi-modal network are more complicated due to the operational characteristics of buses and the interactions between cars and buses. Despite of this complication, studies through simulation for small networks show that a classical MFD still holds for bi-modal urban networks [27], [28]. However, the influence of each mode in the network dynamics and performance is still missing. This relationship, if known, will facilitate the development of control strategies at various levels, e.g. network bus priority or redistribution of urban space [27], [29]. Therefore we aim to investigate how to capture the relationship among the

accumulation of cars and buses, and the traffic throughput or circulating flow of a network. Furthermore, existing methodologies for car-only perimeter control may not be able to optimize network conditions in a multimodal traffic network as it will not consider the buses are more efficient modes due to higher passenger occupancy. To maximize the passenger flow of a network and thus realize the efficiency, we aim to obtain a bi-modal MFD that can capture the dynamics of passenger flow.

The rest of the paper is organized as follows. Section 2 investigates the existence and the properties of a bi-modal MFD by simulation. Section 3 extends the bi-modal MFD modelling from vehicle to passenger flows. Section 4 summarizes the findings and discuss policy indications.

## 2. The Existence of Three-dimensional Macroscopic Fundamental Diagrams: Simulation Findings

In this section, we investigate the relation among accumulation of cars and buses and vehicle flow in bi-modal traffic networks via simulation experiments. We show that a large-scale test site exhibits a city-scale three-dimensional MFD (3D-MFD) relating the accumulation of cars and buses to flow with moderate scatter under different bi-modal demand patterns. We investigate different functions to approximate the shape of the 3D MFD, so that to be integrated in a traffic management framework.

### 2.1 Site and simulated Data

The test site is a 2 km<sup>2</sup> area of Downtown San Francisco including about 100 intersections and 430 links of total 101 lane-km. The number of lanes varies from 2 to 5 lanes and the free flow speed is around 45 km/h. Traffic signals are all multiphase fixed-time operating on a common cycle length of 90 s for the west boundary of the area and 60 s for the rest. The traffic flow in the (bi-modal) network comprises two vehicle classes, i.e., passenger cars and buses. Let us denote by  $n_c$  the accumulation of cars and  $n_b$  the accumulation of buses, and  $Q$  the total network flow (in vehicle per unit time) which is the sum of car and bus flows. For the developed model, the flow  $Q$  in the bi-modal network is considered to be a function of  $n_c$  and  $n_b$  given by

$$Q = Q(n_c, n_b). \quad (1)$$

To obtain the shape of (1) we perform extensive simulation experiments in the test network with time-dependent asymmetric origin-destination tables, starting from different initial compositions of the bi-modal traffic (pairs of  $n_c$  and  $n_b$ ). The initial profile for cars is a typical peak-hour demand with a trapezoidal shape. For buses, the demand is determined by the number of lines and their operational frequency. For the simulation experiments, the test network is modelled via the AIMSUN microscopic simulator. The simulation horizon for each experiment is 5.5 h and pairs of data ( $n_c, n_b$ ) are gathered every 5 min from the simulator. For each 5min interval, total flow  $Q'$  is estimated from the simulator.

Fig.1(a) depicts the projection of the 3D diagram on the ( $n_c, n_b$ ) plane. This projection shows the generated pairs of  $n_c$  and  $n_b$  for different demand patterns. It should be noted that more than 20 runs with different bus frequencies were carried out to generate different mode compositions and obtain the corresponding traffic performance  $Q'$ . Fig.1(b) illustrates the 3D-MFD for bi-modal traffic resulting pattern. As a first remark, Fig. 1(b) confirms the existence of a 3D-MFD like-shape for bi-modal networks, whose exact shape is seen to depend on the accumulation of cars and buses. To enable a better understanding of this figure, Fig. 1(c) displays the contour plot of the 3D-MFD on the ( $n_c, n_b$ ) plane, using an interpolation algorithm to estimate flow in a continuous space of the accumulation plane. The triangle in this figure indicates the bi-modal traffic composition where the network operates close to the maximum throughput of the 3D-MFD. In particular, it captures the “optimal operational region” of bi-modal traffic. City managers and practitioners could seek to derive management strategies to operate at this optimal regime. It can be seen that the flow  $Q'$  decreases monotonically as  $n_c$  and  $n_b$  increases, albeit with different slopes. Remarkably, the slope of buses is higher than the slope of cars. This indicates that effect of an additional bus in the network is much different than an additional car. A simple explanation is that buses make additional to traffic signal stops for passengers, and negatively influence traffic and create stop-and-go phenomena. The figure also depicts critical accumulations of cars  $\tilde{n}_c$  (rising line in the triangular) where  $Q'$  reaches its maximum for different values of  $n_b$ . The slope of the rising line reflects that the capacity to serve cars has to be compromised in order to serve more buses. As a general remark, the 3D MFD can be used by policy makers to exploit the trade-off between the operation of buses and cars and design more sustainable cities. Note also that the maximum value of the network flow occurs for  $n_b = 0$  and  $n_c = 3500$  because of the effect of bus stops. As we will show later, a consideration of different vehicle occupancies for buses and cars and the estimation of network passenger flow will produce a completely different result.

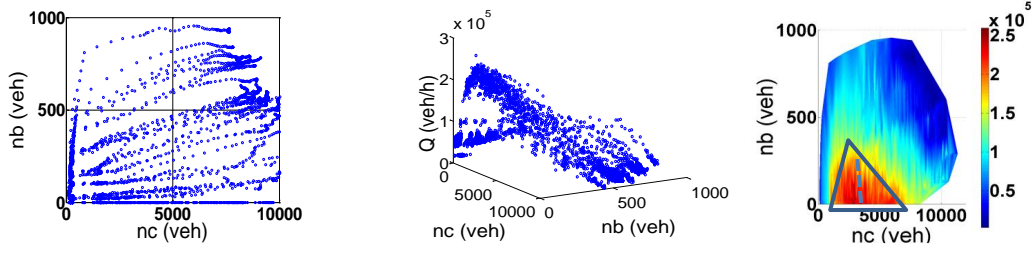


Fig.1. (a) Generated pairs of  $n_c$  and  $n_b$ ; (b) the 3D-MFD points for bi-modal traffic; (c) contour plot of the 3D-MFD after interpolation.

## 2.2 An Exponential Flow Model for Bi-modal Vehicle Traffic

Given that evaluating  $Q(n_c, n_b)$  in (1) for many pairs of  $n_c$  and  $n_b$  is tedious, we propose instead using an exponential flow model that approximates the 3D-MFD in Fig. 1(b). This task is challenging because the ultimate goal is the derivation of a generic 3D-MFD formula with two variables and a few parameters that can be used to improve accessibility in bi-modal traffic networks. To this end, we consider the following exponential flow function for data fitting:

$$Q(n_c, n_b) = a(n_c + n_b)e^{bn_c^2 + cn_b^2 + dn_cn_b + en_c + fn_b} \quad (2)$$

where  $a, b, c, d, e, f$  are model parameters. The parameter values should be specified so as to minimize the deviation of model (2) from the corresponding measured values  $Q'$ . This function can be considered as a generalization of the Drake's exponential function for a 2D single point fundamental diagram. An unconstrained estimation will not be consistent with the physics of traffic and constraints (3) are added. To this end, we estimate the values by Least-Squares parameter estimation for the given simulated data  $Q'$  in Fig. 1(b). The parameter estimation problem is formulated as follows (P1):

$$\min_{a,b,c,d,e,f} Z = \|Q - Q'\|^2$$

Subject to

$$\begin{cases} Q \geq 0 \\ \frac{\partial V}{\partial n_c} \leq 0 & \frac{\partial V}{\partial n_b} \leq 0 \end{cases} \quad (3)$$

where  $V$  is the space-mean speed in the network, PCU is the Passenger Car Unit equivalent value, and  $\mathbf{Q}, \mathbf{Q}'$  are vectors with elements of the model (2) and the simulated data  $Q'$  for each 5-min sample interval, respectively. Variable  $V(n_c, n_b) = QL/(n_c + n_b)$  by definition, where  $L$  is the average link length of the network. The first constraint in (3) guarantees non-negative flows. The second and the third constraint say that the space-mean speed of all vehicles should decrease monotonically as  $n_c$  and  $n_b$  increase.

The parameter estimation problem (P1) is nonlinear and can be readily solved by public or commercial software. The estimated parameters resulting from the optimization problem read:  $a, b, c, d, e, f = 1.95e02, -2.34e-09, 5.28e-07, 6.34e-08, -2.92e-04, -1.50e-03$ .

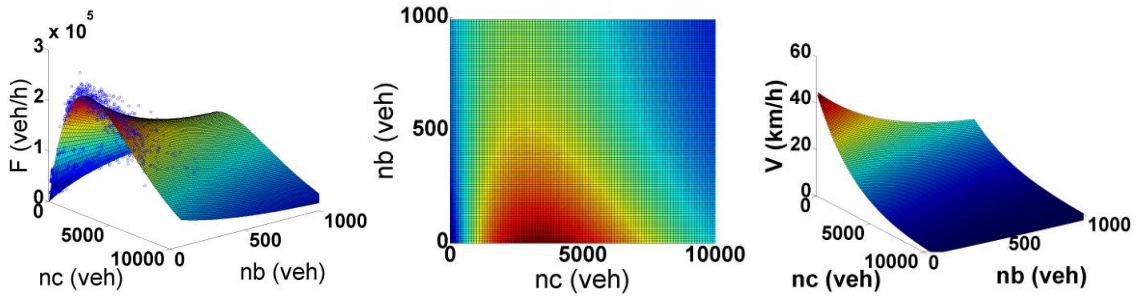


Fig. 2. (a) The approximated 3D-MFD; (b) Contour plot of the 3D-MFD on the  $(n_c, n_b)$  plane. (c) The 3D-MFD relating accumulation of cars and buses with space-mean speed.

Fig. 2(a) illustrates the results of fitting model (2) with the estimated parameters to the simulated data. An R-square value of 0.91 (close to 1) indicates that the resulting 3D-MFD fits well with the data and all physical constraints are satisfied. Note that a slice of the 3D-MFD in Fig. 2(b) for a fixed value of  $n_b$  results to the unimodal MFD of urban traffic. Fig. 2(b) depicts the contour plot of the 3D surface on the  $(n_c, n_b)$  plane. Comparing Fig. 2(b) with Fig. 1(c), we can see that most patterns observed closely matches each other except the area for very high values of buses  $n_b > 600$  due to lack of simulated data. Nevertheless, these states cannot be easily observed in real systems. Moreover, it can be seen that the “optimal operational region” (triangular in Fig. 1(c)) of bi-modal traffic is reproduced in a very similar way. Fig. 2(c) shows the 3D-MFD relating  $n_c$  and  $n_b$  with the space-mean speed  $V$  in the network.

### 3. The Derivation of a Three-dimensional Macroscopic Fundamental Diagrams for Passenger Flow

Given the 3D-MFD (2) of a network with cars and buses, incoming flow can be controlled at the boundary of the network in order to direct the network operates at its “optimal operation region”. Existing methodologies for car-only perimeter control can be found in [24], [25], [30] and elsewhere. Based on this MFD, however, it is possible that a controller would always try to restrict bus flow from entering the network. This is due to the monotonic relation between bus accumulation  $n_b$  and the flow  $Q$ . From a passenger mobility perspective, this control strategy cannot optimize network conditions as it will not consider the buses are more efficient modes, due to higher passenger occupancy. To maximize the passenger flow of a network and thus realize the efficiency of a multimodal network, we shall need a bi-modal MFD that can capture the dynamics of passenger flows. In this section, we describe a derivation of the analytical form of the passenger flow 3D-MFD based on the vehicle flow 3D-MFD.

Denote  $P$  the passenger flow in the bi-modal network, with  $n_c$  and  $n_b$ ,  $P = P(n_c, n_b)$ . Denote  $h$  the average number of on-board people per vehicle, the occupancy. We assume that car occupancy  $h_c$  is constant  $h_c = 1.3$ , while bus occupancy  $h_b$  with a model proposed in [27], as a function of the dwell time. Denote speed of car  $v_c$  and bus  $v_b$ , the flow of cars  $Q_c$  and buses  $Q_b$ . By definition, total passenger flow  $P$  can be written by (4):

$$P = h_c Q_c + h_b Q_b \quad (4)$$

Given the analytical form of  $Q$  in (2), we try to estimate  $Q_c$  and  $Q_b$  for each mode by  $Q$ ,  $n_c$  and  $n_b$ . To this end, we first consider that  $V = (v_c n_c + v_b n_b)/(n_c + n_b)$  and:

$$Q = Q_c + Q_b = (v_c n_c + v_b n_b)/L \quad (5)$$

Then, to obtain  $v_b$  as function of  $v_c$ , we utilize the speed model proposed in [27]:

$$v_b = v_c \frac{s}{s + \tau v_c} \quad (6)$$



where  $s$  is the average distance between successive bus stops and  $\tau$  is the average dwell time at a bus stop. The values of  $L$  and  $\tau$  are network specific. Assume first-order approximation in (6), the linearization yields:

$$v_b \cong \theta v_c + \beta \quad (7)$$

where  $\theta$  and  $\beta$  are parameters. Introducing (7) in (5), we can solve (5) with  $v_c$  as the unknown variable and obtain the analytical form of  $v_c$ . Given the analytical form of  $Q_c = v_c n_c$  and  $Q_b = v_b n_b$ , then  $P$  can be readily derived by combining (4) as follows:

$$P = h_c n_c \frac{QL - \beta n_b}{(n_c + \theta n_b)} + h_b n_b \left( \frac{QL - \beta n_b}{(n_c + \theta n_b)} \theta + \beta \right) \quad (8)$$

## 4. Discussion

In this paper, we extended the single-mode Macroscopic Fundamental Diagram model to a bi-modal (bus and cars) one, with the consideration of passenger flows in addition to vehicle flows. We investigated the relation between the accumulation of cars and buses, and the vehicle flow throughput of the network via a 3D-MFD. This 3D-MFD was developed and parameterized for both vehicle throughput and passenger throughput. We have shown via simulation experiments that: (i) an exponential family function fits well the data points, (ii) the network's vehicle throughput decrease monotonically by increasing the number of buses serving in the network. We also derived the analytical form of a 3D-MFD for passenger flow. The findings of this paper are promising because the concept of a 3D-MFD can be used: (i) to monitor traffic performance in bi-modal networks, and traffic flow dynamics can be predicted given the current state of the two modes, and (ii) towards the development of simple control policies in such a way that maximizes the bi-modal network vehicle flow or passenger throughput. Moreover, policy makers can adjust management measures to operate at different mobility levels as expressed by the MFD in Fig. 2(b). An extended version of this paper will be available soon where more detailed information on the 3D-MFD can be found. On-going work investigates how perimeter control of cars can improve the system operation and decrease total passenger delays.

## Acknowledgement

This research was financially supported by the Swiss National Science Foundation (SNSF)

grant # 200021-132501.

## References

- [1] C. Daganzo and M. Cassidy, "Effects of high occupancy vehicle lanes on freeway congestion," *Transport Research Part B*, Vol. 42, No. 10, pp. 861-872, 2008.
- [2] J. Li, M. Song and W. Zhang, "Planning for bus rapid transit in single dedicated bus lane," *Transportation Research Record*, Vol. 2111, pp. 76-82, 2010.
- [3] P. Site and F. Filippi, "Service optimization for bus corridors with short-run strategies and variable vehicle size," *Transport Research Part A*, Vol. 32, No.1, pp. 19-38, 1998.
- [4] A. Tirachini and D. Hensher, "Bus congestion, optimal infrastructure investment and the choice of a fare collection system in dedicated bus corridors," *Transport Research Part B*, Vol. 45, No. 5, pp. 828-844, 2011.
- [5] M. Mesbah and G. Currie, "Optimization of transit priority in the transportation network using a genetic algorithm," *IEEE Transactions on Intelligent Transportation Systems*, Vol. 12, No. 3, pp. 908-919, 2011.
- [6] M. Eichler and C. Daganzo, "Bus lanes with intermittent priority: Strategy formulae and an evaluation," *Transport Research Part B*, Vol. 40, No. 9, pp. 731-744, 2006.
- [7] E. Christofa, K. Aboudolas and A. Skabardonis, "Arterial traffic signal optimization: A person-based approach," in *Proc. 92nd Annual Meeting of the Transportation Research Board*, Washington, D.C., USA, 2013.
- [8] Bureau of Public Roads, "Traffic Assignment Manual," U.S. Dept. of Commerce, Urban Planning Division, Washington D.C., USA, 1964.
- [9] K. Tuerprasert and C. Aswakul, "Multiclass cell transmission model for heterogeneous mobility in general topology of road network," *Journal of Intelligent Transport Systems: Technology, Planning, and Operations*, Vol. 14, No. 2, pp. 68-82, 2010.
- [10] J. Godfrey, "The mechanism of a road network," *Traffic Engineering and Control*, Vol. 11, No. 7, pp.323-327, 1969.
- [11] H. Mahmassani, J. Williams and R. Herman, "Performance of urban traffic networks," in *Proc. 10th Int. Symp. on Transportation and Traffic Theory, Amsterdam, The Netherlands*, 1987, pp. 1-20.
- [12] C. Daganzo, "Urban gridlock: macroscopic modeling and mitigation approaches," *Transportation Research Part B*, Vol. 41, No. 1, pp. 49-62, 2007.
- [13] N. Geroliminis and C. Daganzo, "Existence of urban-scale macroscopic fundamental diagrams: some experimental findings," *Transportation Research Part B*, Vol. 42, No. 9, pp. 759-770, 2008.
- [14] A. Mazlounian, N. Geroliminis and D. Helbing, "The spatial variability of vehicle densities as determinant of urban network capacity," *Philosophical Transactions of Royal Society A*, Vol. 368, No. 1928, pp. 4627-4648, 2010.
- [15] C. Daganzo, V. Gayah and E. Gonzales, "Macroscopic relations of urban traffic variables: bifurcations, multivaluedness and instability," *Transportation Research Part B*, Vol. 45, No. 1, pp. 278-288, 2011.
- [16] C. Daganzo and N. Geroliminis, "An analytical approximation for the macroscopic fundamental diagram of urban traffic," *Transportation Research Part B*, Vol.42, No. 9, pp. 771-781, 2008.
- [17] N. Geroliminis and B. Boyaci, "The effect of variability of urban systems characteristics in the network capacity," *Transportation Research Part B*, Vol. 46, No. 10, pp.1607-1623, 2012.
- [18] C. Buisson and C. Ladier, "Exploring the impact of homogeneity of traffic measurements on the existence of Macroscopic Fundamental Diagrams," *Transportation Research Record*, Vol. 2124, pp. 127-136, 2009.
- [19] Y. Ji, W. Daamen, S. Hoogendoorn, S. Hoogendoorn-Lanser, and X. Qian, "Macroscopic fundamental diagram: investigating its shape using simulation data," *Transportation Research Record*, Vol. 2161, pp. 42-48, 2010.
- [20] N. Geroliminis and J. Sun, "Properties of a well-defined macroscopic fundamental diagram for urban traffic," *Transportation Research Part B*, Vol. 45, No. 3, pp. 605-617, 2011.
- [21] M.Saberi and H. Mahmassani, "Exploring properties of network-wide flow-density relations in a

- freeway network,” *Transportation Research Record*, No. 2315, pp. 153-163, 2012.
- [22]Y. Ji and N. Geroliminis, “On the spatial partitioning of urban transportation network,” *Transportation Research Part B*, Vol. 46, No. 10, pp. 1639-1656, 2012.
- [23]V. Knoop, S. Hoogendoorn and H. van Lint, “The impact of traffic dynamic on the Macroscopic Fundamental Diagram,” in *Proc. 92nd Annual Meeting of Transportation Research Board*, Washington D.C., USA, 2013.
- [24]M. Keyvan-Ekbatani, A. Kouvelas, I. Papamichail and M. Ppapegeorgiou, “Exploiting the fundamental diagram of urban network for feedback-based gating,” *Transport Research Part B*, Vol. 46, No.10, pp. 1393-1403, 2012.
- [25]N. Geroliminis, J. Haddad and M. Ramezani, “Optimal Perimeter Control for Two Urban Regions with Macroscopic Fundamental Diagrams: A Model Predictive Approach,” *IEEE Transactions on Intelligent Transportation Systems*, Vol. 14, No.1, pp. 348-359, 2012.
- [26]N. Zheng, R. Waraich, K. Axhausen and N. Geroliminis, “A dynamic cordon pricing scheme combining the Macroscopic Fundamental Diagram and an agent-based traffic model,” *Transportation Research Part A*, Vol. 46, No. 8, pp. 1291–1303, 2012.
- [27]N. Zheng and N. Geroliminis, “On the distribution of urban road space for multimodal congested networks,” in *Proc. 20th Int. Symp. on Transportation and Traffic Theory*, Noordwijk, the Netherlands, 2013.
- [28]E. Gonzales, C. Chavis, Y. Li and C. Daganzo, “Multimodal Transport in Nairobi, Kenya: Insights and Recommendations with a Macroscopic Evidence-Based Model,” in *Proc. 90th Annual Meeting Transportation Research Board*, Washington, D.C., USA, 2011.
- [29]E. Gonzales and C. Daganzo, “Morning commute with competing modes and distributed demand: User equilibrium, system optimum, and pricing,” *Transportation Research Part B*, Vol. 46, No. 10, pp. 1519-1534, 2012.
- [30]K. Aboudolas and N. Geroliminis, “Feedback perimeter control for multiregion and heterogeneous congested cities,” in *Proc. 92<sup>nd</sup> Annual Meeting of Transportation Research Board*, Washington D.C., USA, 2013.